

A Novel Portable Surface Plasmon Resonance Based Imaging Instrument for On-Site Multi-Analyte Detection

Sara Rampazzi, Francesco Loporati,
Giovanni Danese, Nelson Nazzicari
Dip. di Ing. Industriale e dell'Informazione
Università degli Studi di Pavia
via Ferrata 1, Pavia, Italy
Email: sara.rampazzi01@universitadipavia.it,
{francesco.leporati, gianni.danese}@unipv.it,
nelson.nazzicari@gmail.com

Lucia Fornasari, Franco Marabelli
Dip. di Fisica "A. Volta"
Università degli Studi di Pavia
via Bassi 6, Pavia, Italy
Email: {franco.marabelli,
lucia.fornasari}@unipv.it

Andrea Valsesia
Plasmore s.r.l.
via G. Deledda, Ronco (Varese),
Italy
Email:
andrea.valsesia@plasmore.com

Abstract—In the last decade the need for portable Surface Plasmon Resonance (SPR) biosensors capable of on-site simultaneous multiple assays increased steadily. Several devices are available affected, however, by limitations in terms of costs, size, complexity and portability.

A compact low-cost SPRi biosensor based on a novel method for multi-analyte detection is presented.

The prototype consists of a nanohole array biochip integrated with a compact optics and an elaboration system. A CMOS image sensor captures reflected light from the biochip surface irradiated by a 830 nm LED. The entire system is managed by an ARM9 processor.

The biosensor was able to detect a $\sim 10^{-5}$ RIU change in the refractive index without analyte receptors at a glycerol concentration equal to 0.2%. Results are available in 14 seconds on LCD display and immediately stored to external SD memory. Preliminary experiments confirmed the strong biosensor's usability in a wide range of applications and fields.

I. INTRODUCTION

THE last 30 years have witnessed a rapid growth in the use of biosensors in both research and practical applications. Molecular biology, biotechnology together with genetic, protein and pharmaceutical engineering are the most common applications fields of these devices. This trend is due to technological innovations that increased their sensitivity, versatility and integrability within microprocessor-based electronics. However, most of these powerful instrumentations are only used in specialized laboratories because of their high cost. In particular the biosensors based on Surface Plasmon Resonance (SPR) have been developed into a very useful technology applications due to their high sensitivity but the majority of this devices are only for research use [1]. The Surface Plasmon Resonance is an optical phenomenon that offers specific advantages in bio-molecular studies. First of all, it is label-free technique that allows real-time direct detection of molecular binding, enabling the determination of their concentration during this interaction without the need for fluorescence or radioisotope labelling. Moreover, it can be applied for kinetic measurements and to perform simultaneous assays on the

same biochip (SPR *imaging*-SPRi). Antibody–antigen interactions, peptide/protein–protein interactions, DNA hybridization conditions, biocompatibility studies of polymers, biomolecule–cell receptor interactions and DNA/receptor–ligand interactions have been well analyzed by means of this approach [1]. However the complex fabrication procedure to make the measures more accurate and fast, increases their cost (more than 10,000\$) and their size (most of them are benchtop instruments). This limited the diffusion of SPR biosensors outside the industrialized countries, hampers significant improvement of hygiene and environmental conditions. We present a novel portable SPRi biosensor based on a nano-structured crystal biochip developed by [2]. It is a multi-parametric system for biological and molecular interaction monitoring using the Localized Surface Plasmon Resonance (LSPR) phenomenon. Our device allows to detect the presence and the amount of specific target molecules (called *analytes*) in a liquid samples without the use of an external computation device (like computer). The potential applications fields of this instrument are enormous: biochemical and chemical assays in medicine for diagnostic and monitoring of the patients, for water and soil pathogen detection, for process control in pharmaceutical chemistry and drug and food monitoring for toxins detection. This biosensor allows the acquisition of the light reflected from crystal's surface irradiated at a specific wavelength; the crystal is a biochip in which micro-spots of antibodies deposited on the surface are sensitive to different analytes to be identified in the sample. The estimate of the presence and concentration of the searched analytes is available in about 14 seconds on a LCD display and stored in a MicroSD card. This work will focus on the development of the prototype together with the implementation choices to realize a compact low-cost and low-power consumption SPR device. The Linux kernel-based modules conceived for the images acquisition and elaboration are also discussed with a novel method to identify analytes presence and amount. Finally, the detection capabilities of the device are provided

measuring bulk refractive index changes in glycerol solutions at different concentrations.

II. INTEGRATED SPR SYSTEM AVAILABLE

The most common commercial SPR biosensors in the last decades are generally based on the Kretschmann's configuration where a laser source radiates a glass prism covered with a thin metal film. However this simple technique features sensitivity limitation for low molecular weight analytes [3]. The technology improvement allowed new approaches to SPR for increase the sensitivity (plasmon waveguide resonance, channel parallel array, etc...) but this made biosensors more expensive with less attention to an integrated, portable, low-cost and low-power consumption device.

Only recently the market geared toward the fabrication of compact instrumentations for the simultaneous detection of one or multiple analytes and this implied the miniaturization of each system's components and the develop of new SPR technology solutions.

The most best known example of marketed compact SPR devices is Spreeta (Texas Instruments, USA). These instruments measure approximately 1.5 cm x 0.7 cm x 3 cm and consist of a plastic prism assembled on a PCB that contained an infrared LED, a linear diode array detector and a non-volatile memory [4]. The LED light beam through a plastic sheet polarized, strikes a glass chip coated with a gold layer. The SPR waves produced are captured by the diode array detector. Spreeta cost is about 50\$ [5] with a resolution of 5×10^{-6} RIU [4]. Spreeta, however, requires an integration with external fluidics systems and suitable elaboration units to manage acquisition and analysis. Another limitation is due to temperature which significantly affects the refractive index, requiring a control system to keep it constant.

Many research works exploit Spreeta technology to develop compact multi-analyte SPR instruments. Chinowsky's describes a semi-automatic 24-channel system for toxin identification, called "SPIRIT". This lunchbox-size instrument weighs approximately 3 Kg and is made by eight replaceable three-channels Spreeta 2000, a 1 MHz analog-to-digital converter and a DSP microcontroller [6].

The device also contains a touch-screen LCD display and a flash memory for data storage, however needs a PC connection for long-term reaction monitoring and displaying of all the 24 channels.

Another low cost biosensor based on Spreeta is described by Hu et al. in 2009. This bioanalyzer uses a three-channels Spreeta TSPR1K23 and three processors for temperature control, data analysis and display control [7]. Similarly to the previous one, this instrument needs a high precise temperature sensor and uses a PID algorithm control for temperature regulation. Only three analytes for sample are detectable and its considerable weight makes it unsuitable to perform on-site assays also in unfavourable environments.

In addition to Spreeta devices, different approaches can be considered to optimize the Kretschmann configuration. For example, in 2010 Cai et al., developed a portable SPR

biosensor based on the image scanner chip LM9833. A wedge shape laser beam radiated a cylinder prism and the reflected light was captured by a CCD camera driven by the image scanner [8]. A single board industrial PC was used to provide the analysis results featuring about 1 Kg weight. The refractive index sensitivity was about 6×10^{-5} RIU, however this device required 30 minutes of baseline stabilization before each analysis.

A palm-size biosensor based on light source modulation was developed by Shin et al. in 2010. The beam of a diode laser was modulated by a rotating mirror and the reflected light was captured by a CMOS [9]. The refractive index resolution was quite interesting (about 2.5×10^{-6} RIU at a 3% glycerol concentration) but this device requires temperature control and PC for elaborating signals via LabVIEW code. It also suffers from mechanical solicitations that require an highly synchronization between the frame rate of the CMOS image sensor and the revolution speed of the mirror, to limit the noise level due to the present artefacts that compromise the portability.

Another solution has been adopted by Wichert et al. His team used the Plasmon Assisted Microscopy of Nanoobject (PANOMO) technique with FPGA technology and CCD camera. However it allows to detect only specific viruses [10].

In parallel to Kretschmann-based systems, optical fibers and waveguide structures have been used to fabricate miniaturized biosensors (Tzyy-Jiann et al., 2004). The use of waveguides is similar to Kretschmann configuration since by coating the fiber with a metal film, each reflection of light, corresponds to the reflection spectrum of a Kretschmann configuration. However this solution requires a careful choice of the fiber type and complex design and assembly that increase fabrication costs [11].

Another technique uses diffraction gratings to couple the plasmon resonance with the optical wave. In 2009 a 4-channel compact biosensor has been presented by Piliarik et al. [12] and one year later Vala and his team developed a device capable of simultaneous detection of 10 analytes [13]. The beam reflected by the grating is collimated by lens and captured by a CCD camera that evaluate the average over 50 frames by onboard electronics and transmits it via USB. Although featuring both a high resolution (3×10^{-7} RIU and 6×10^{-7} RIU respectively when the RI index change of a NaCl water solution is 0.00312 in both cases) and compact size they need an external PC for elaborating images.

In the last years the significant progress in nanotechnology have led to remarkable results in the study of Localized Surface Plasmon Resonance (LSPR) phenomenon. The use of nano-scaled metallic structures provides a new route to overcome the limitations described before, allowing to perform SPRi (see Section 3).

We describe here the design, implementation and characterization of a new SPR imaging biosensor based on LSPR with a novel efficient analysis method overcoming temporal light variations and noise. This approach considers two control regions in the sensible area of the nanostructured

biochip and one macro area where the sample will be injected. The entire system doesn't require the use of external PC for the elaboration and does not have moving parts or additional temperature control sensor.

The goal of our research is to develop a palm-size low-cost instrumentation that allows relatively untrained user to perform rapid multiple simultaneous assays outside of specialized laboratory for a wide range of applications.

III. PRINCIPLES OF LOCAL SURFACE PLASMON RESONANCE AND IMAGING

Surface plasmons (SP) are longitudinal charge density waves along the interface between a metal and a dielectric [14]. When a P-polarized beam radiates the interface between the media at a specific resonant angle and the wave component parallel to the surface matches the wavevector evanescent component of the plasmonic mode, it can resonantly couple and excite the mode. The coupling to the plasmonic mode results in an energy loss and then in an intensity reduction of reflected light.

In a SPR biosensor, receptor molecules are chemically immobilized on the metal surface. Therefore, when the target substance diluted in a liquid sample reacts with the receptor, a change in the resonance conditions is observed. Analyte/receptor reaction produces a refractive index change close to the surface which can be related to analyte concentration [14]. Typically, SPR system maximum sensitivity is about 10^{-7} RIU [15].

The rapid development of nanotechnologies, stimulated the study of the physical properties of metallic nanostructured, whose optical response can be exploited to improve surface plasmon resonance technique.

Metallic nanostructures support charge density oscillations called *Localized Surface Plasmons* (LSPs). Metal conduction electrons can be excited through a light beam to a collective oscillation state with a specific resonant frequency that depends on the size, shape, composition, dielectric properties of the material and spatial distributions of nanoparticles [16, 17]. Haes and Van Duyne, in 2004, demonstrated that LSPR has a sensitivity which is approximately equivalent to traditional SPR techniques. As a consequence, SPR systems can be miniaturized without significant sensitiveness loss.

The strongly dependence on the type of metal, shape and size of nanostructures, pushed researchers to identify the optimal design improving optical sensing.

In the last 10 years, significant results have been reached: basically, two possible approaches can be exploited.

In the first, metallic nanoparticles are immobilized on a glass substrate, while in the second one a glass substrate is covered with a metal thin film in which a periodic array of nanoholes is carried out [18]. A significant difference between these structures was explored in 2009 by Parsons et al. who demonstrated that the optical response of nanoparticles is independent of interparticle separation, while the response in periodic subwavelength nanohole arrays is largely dependent on interhole separation [19]. In

particular, experiments highlighted that the peaks of transmittance spectrum were correlated to the period between nanoholes and that the amount of transmitted light was greater than that predicted by the classical theory. This phenomenon is called *Extraordinary Optical Transmission* (EOT) effect [20].

The possibility of producing nanostructured plasmonic surfaces with versatile and simple techniques such as lithographic one, makes this approach more compatible with the SPR imaging method.

An imaging SPR biosensor allows to detect multiple types of molecules simultaneously on a single chip. The binding interaction between the receptor substances attached to the metal surface and the molecules to be detected is monitored by a CCD or CMOS camera. The simplicity of the entire structure with no moving parts and the use of nanoholes array structure allows to overcome the difficulty to develop a multi-channel efficient biosensors for high-throughput analysis [18].

IV. INSTRUMENT DESIGN

According to the previously described state-of-the-art, our device combined the high performance of nanohole biochip with an embedded elaboration system to realize a new portable SPRi biosensor.

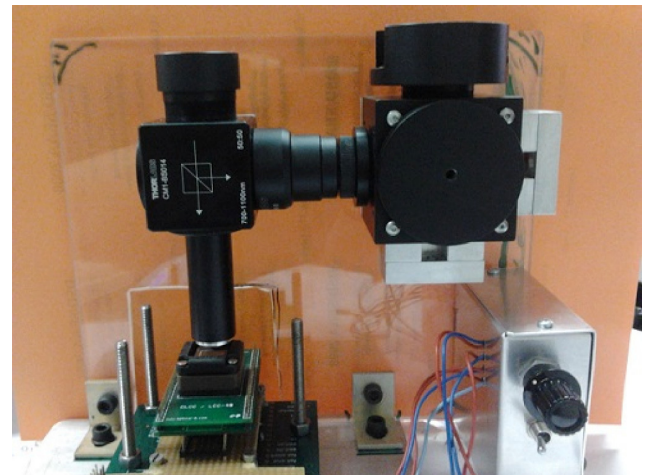


Fig 1. The biosensor prototype

The developed prototype showed in figure 1 is composed by two main parts: a bio-sensing surface with optical set up and an electronic unit for images acquisition and data elaboration.

A. Bio-sensing device

In a typical EOT biosensor, a collimated light beam is focused on the sensing region and the reflected light is captured by a spectrometer.

Many researches about EOT sensors performed by [21, 22, 23] demonstrated that their refractive resolution measured is similar to conventionally SPR system sensitivity ($\sim 10^{-6}$ RIU).

For our prototype we used a nanostructured biochip realized by [2] in 2011. Its sensitive surface is composed of an nanoholes array embedded in a gold film [2].

The chips were produced through a colloidal lithographic technique: a glass substrate was covered by plasma polymerized poly-acrylic acid via plasma enhanced chemical vapour deposition (PE-CVD) and a subsequent layer of polystyrene beads (PS) are deposited on the top of the ppAA. In order to form a grating structure of a regularly spaced pillars, the layers were exposed to oxygen plasma *etching*. A gold layer is deposited on the nanostructure by vapour deposition to fill-in the gaps between pillars. Then, the residual PS mask is removed using lift-off by an ultrasonic bath in ultra-pure water. The obtained biochip features periodic gold cavities with shapes that widen to their bottom. The opening width is in the range of 50-250 nm, the bottom of 100 to 450 nm with a cavity periodicity of 200 to 1000 nm [2].

A recent work performed by Giudicatti et al. shows that this particular asymmetric pillars geometry increased the electric field in the cavities where the analytes receptors are located, contributing to strengthen the EOT effect and increasing the sensitivity in the order of 10^{-5} RIU [2].

Furthermore, the reflectance measured from the glass side of the biochip is sensitive to the refractive index at the opposite side. This characteristic allows to measure the optical

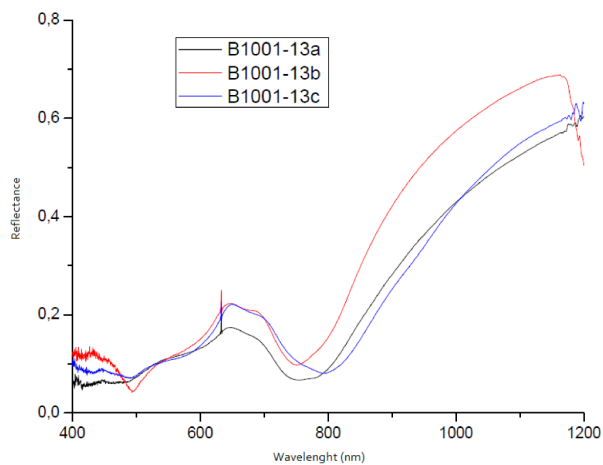


Fig 2. Reflectance spectra of different biochip used on trials. The minimum of reflectance is located in the 700-850 nm region.

response without expensive optical apparatus and collimated light source [24].

We studied the biochip reflectance spectra to identify the correct signal region where the resonance occurs. The trend showed in figure 2 highlights that the sensible region is located between 700 and 850 nm. Accordingly to this study we chose a LED light source (Vishay TSHG8200 IR LED) with 830 nm wavelength peak.

The light beam passes through one cube beamsplitter (CM1-BS015 by Thorlabs Inc.) and an achromatic lens (AC127-025-b by Thorlabs Inc.) to ensure the proper uniform

irradiation of the sample minimizing aberrations. Run-time, the sensor is orientated so as the light beam illuminates the cavities from the widest bottom side while the detector captures the reflected light as shown in fig. 1.

The simple lithographic techniques together with no complex optics required allow the biochips mass production, providing an efficient solution for low-cost SPR biosensors fabrication.

B. Electronic unit

The electronic platform is composed by the image detector and the elaboration system. For capturing the reflected light of the biochip surface, we selected an APS CMOS. Since 1995, the increasing interest in CMOS image sensors was related to their design flexibility, reduced costs and low power consumption. The Active Pixel Sensor (APS) CMOS differs from the traditional passive CMOS for its robustness to noise due to the pixel amplification. Studies demonstrated that APS CMOS performance is comparable to their CCD equivalent [25]. We choose the MT9M001C12STM (Aptina Corporation), a monochromatic 1024x1280 pixel APS CMOS with a quantum efficiency (QE) suitable for our purposes. A 10 bit onboard analog-to-digital converter (ADC) codifies each pixel directly to the elaboration unit responsible for image processing and controlling the sensor via I²C protocol.

In particular this unit acquires each image by the sensor, elaborates them, shows the analysis results on a LCD display and stores all the information on a MicroSD. This kind of approach requires a low power consumption and low costs flexible architecture for the portability and robustness of the instrument. For these reasons we selected the ARM9 family (AT91SAM9260 Atmel Corporation). The processor is mounted on the SAM9-L9260 development board developed by Olimex Ltd. The board features 64 MB SDRAM and 512 MB Nand Flash, an Ethernet 100 Mbit controller and a SD/MMC card connector directly linked to the processor.

V. SOFTWARE PLATFORM

The primary tasks of the realized software platform are to ensure the communication between all the devices components, run the analyte detection algorithm and interact with the end user for the trials configurations and results visualization. These services must be managed by a specific software designed to optimize the performance but easily modifiable to add or change functionalities.

Since many years Linux has become an efficient solution to perform these tasks. It is a Unix-like, modular and multitasking operating system that supports a wide range of devices and configurations [26]. Furthermore, the open-source code availability allows software designers to modify the code according to their own needs improving costs and efficiency.

A typical Linux operative system scheme is a monolithic kernel where user applications run in the user space and operate on a virtual address to protect the internal memory.

The users program cannot directly access the system hardware but can request services to kernel by primitive system calls.

A specific *bootloader* at the starting time, initializes the hardware, defines the memory space map, enables the MMU (Memory Manage Unit) if present, and configures the processor for loading the operating system's kernel.

In our case, the onboard bootloader U-boot (<http://www.denx.de/wiki/U-Boot/SourceCode> with the Olimex board patches available on https://www.olimex.com/Products/ARM/Atmel/_resources/u-boot-olimex-patches-20090717.tgz) has been used to initialize the ARM9 processor.

A. Linux-based Operating System

The basis of our prototype is a minimal operating system called SSW realized by A. Rubini in 2010 and release under GNU General Public License (GPL). It is a small Linux-based operating system derived from THOS (www.gnudd.com/wd/thos.pdf). It is conceived for several family processors that we modified and extended to include the biosensor configuration and management.

The SSW operating system uses ARM9_v5 architecture composed by the MMU initialization, exceptions handlers, a simple I/O model, the module interface, and the tasks scheduler.

The Memory Management Unit controls the memory access and translates virtual to physical addresses. In our operating system the 4 GB virtual memory is divided in 1 MB sections with no cache [27].

The ARM exceptions are implemented through a vector table with branch instructions to specific code that saves registers and performs the right operations. The seven types of exceptions supported drive the processor in specific privileged modes accessing to different registers, stack and handler.

The kernel modules are initialized through a suitable initcall routine. At the system boot, modules set up is performed according to a specific hierarchy. At first, the modules with no dependencies like the serial port and the interrupt controller. Then, the architecture modules like the memory controller and timers, the peripheral devices and lastly the tasks modules.

The interface to modules is defined by two suitable macros *request()* and *provide()*.

The application programs that use modules can be activated periodically or not. A simple Round Robin scheme was implemented for the tasks scheduling. The tasks are kept in two doubly linked lists: one for the running ones and one for the idle ones. The initialization function prepares the first set up parameters (activation time, periodic execution or not, other parameters) and put the task in the idle list, from which it will be selected according to the Round Robin scheduling. This approach is a simple timeline-based scheduling where the system design chooses the activation time and period for each task. The scheduler temporization is implemented using

timer interrupts. Specifically, a processor timer is programmed to generate an interrupt signal every 10 ms.

B. Biosensor device drivers and application

We extended the previously described operative system with an hierarchical collection of modules and drivers that use the simple GPIO pins to peripherals management and an application program to allow the biosensor utilization. The AT91SAM9260 configuration drivers, the acquisition interface for the image sensor, the LCD display and SD/SDHC modules are implemented using the minimal hardware and configuration required. This approach assures the software reusability with different hardware or other Linux-based operating systems with the possibility to easily add or change functionalities.

The biosensor application program realized configure the initial parameters of the biosensor, sets the trials periodicity and the number of images acquired, invoke the modules needed and provide to the end users the analysis results.

The main part of the described software platform is the communication management between the board, the image sensor, the display and the external SD memory.

The image sensor device uses I²C protocol to read and write the internal sensor registers. These registers control various features like black level calibration, integration time for the pixels and readout modes of the sensor. The data output is controlled by three different signals: the pixel clock, the line valid and the frame valid.

The image data is read out sequentially. Each 10 bit pixel is ready on the falling edge of the pixel clock signal when both the line valid and frame valid are activated.

We developed specific modules for the images acquisition using the GPIO processor interface via a simple PWM signal. Each image is elaborated in about 4 seconds by the application software that makes available on LCD display the trial results and stores on SD memory in 14 seconds. A FAT16 partition is created on external memory during the application software boot to neatly memorize them on specific files.

VI. ANALYTES DETECTION METHOD

The goal of the biosensor is to provide a robust detection of the presence and amount of the target analyte on a liquid sample. This required a fast and efficient identification algorithm. The conducted research about the raw pixels of the images has highlighted temporal fluctuations of the light intensity acquired from the sensor that significantly influences the analysis results. In particular, the main effect is an upward trend of the pixels grey level average observable in figure 3.

Experiments conducted with different black level calibration, integration times and LED sources, demonstrated that not homogeneous light diffusion and photons accumulation on the sensor during long time exposition are the major causes of this phenomenon.

The study also revealed a saturation level not time-predictable, but affecting each image region.

To overcome the instability we used the pixel average ratio between specific image areas.

The approach is to normalize the grey level pixel average of the area where the antibodies are deposited, with the average of an external area of the same surface designed as control region where there is no active molecules.

With this method when the antibody-analyte reaction takes

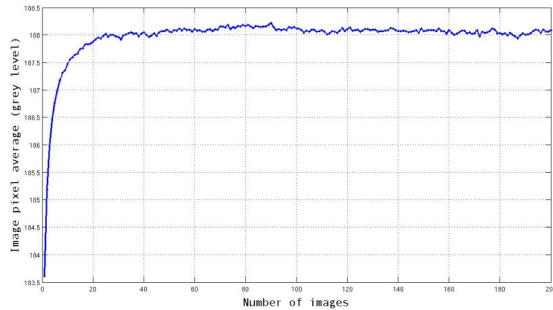


Fig 3. Gray levels pixel average measured during 200 images acquisition without antibodies on the biochip surface. After 50 images the light intensity reaches a saturation level.

place, the different light intensity measured is only influenced by the LSPR phenomenon without light aberrations.

Figure 4 a) shows the pixel average ratio of three regions of the biochip surface without immobilized antibodies. Two areas (2 and 3) are used as control regions and in the third distilled water was injected after 10 images acquired. The normalization applied eliminates the previously described

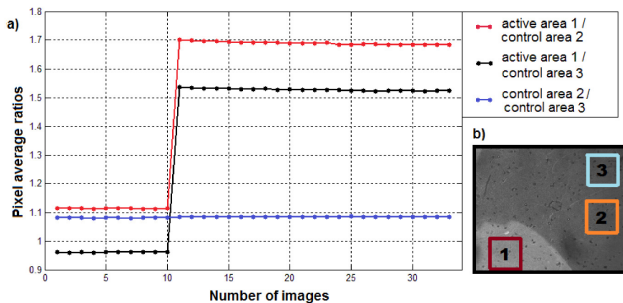


Fig 4. (a) Trend of pixel average ratio between three biochip regions without antibodies. After the tenth image distilled water was injected on the area 1; (b) 128x128 pixels areas used for the experiment. Areas 2 and 3 are control region.

instability and the ratios values are perfectly constant before and after the water injection.

It can be also seen the different average ratios measured are independent of each other since relative to biochip regions with different illumination. All the relevant information is included on the deviation before and after the water injection that corresponds to refractive index change due to LSPR phenomenon.

On this basis, we used the time derivative of average ratio as a suitable measurement of the refractive index variation on the biochip surface. Fig. 5 illustrates the average ratios and time derivatives of three areas, two control regions (area 1 and area 2) and a sample area (area 3). Distilled water was used as reference baseline, then (after 14 acquired images) a 5% glycerol solution was injected on the sample area.

The figure shows the time derivative change due to the refractive index variation on the sample area. Peak position and ratio increase of course correspond perfectly.

Such as in previous case (injection on area 1), we observed a change in the measured ratio according to refractive index variation of the biochip surface in contact with the sample. The developed algorithm measures the amplitude of the time derivative peak that is compared with a specific refractive index calibration curve in the internal memory of the processor. The obtained value is used to define the target analyte concentration in a sample.

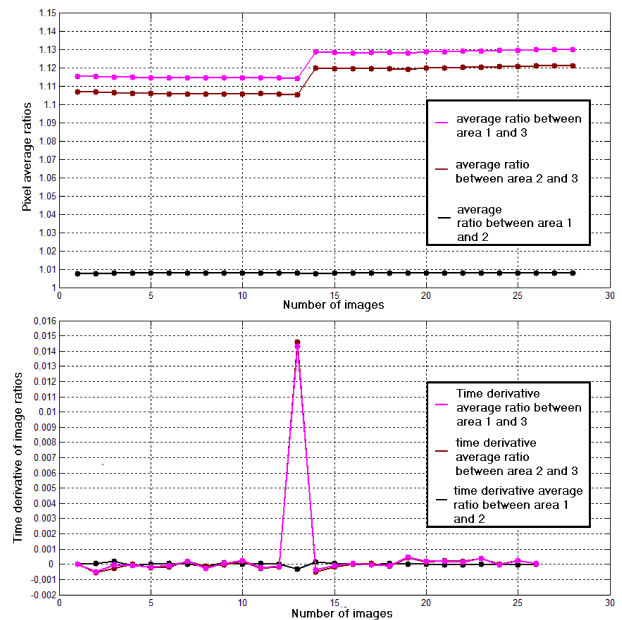


Fig 5. Pixel average ratio and time derivative when the sample area 3 is filled with distilled water (refraction index = 1.333) and then with a glycerol solution with concentration 5% (refraction index = 1.339).

VII. RESULTS AND DISCUSSION

A. Sensitiveness of the biosensor

In order to evaluate the biosensor sensitiveness to changes in refractive index of bulk solutions and define a preliminary calibration curve for the algorithm developed, we prepared glycerol solutions with different concentrations (0.2% - 5%). The biochip surface is subdivided in three rectangular areas (150x800 pixels), two taken as control regions and one selected region where the solutions were injected. Distilled water is flowed on selected region as stable baseline reference for a few number of images (5-10) and

then the glycerol solution was introduced. The acquisition session relative to each concentration took 20 minutes.

Fig. 6 shows the linear correlation between the peak amplitude of the time derivative of average gray level pixel ratio at the various glycerol concentrations.

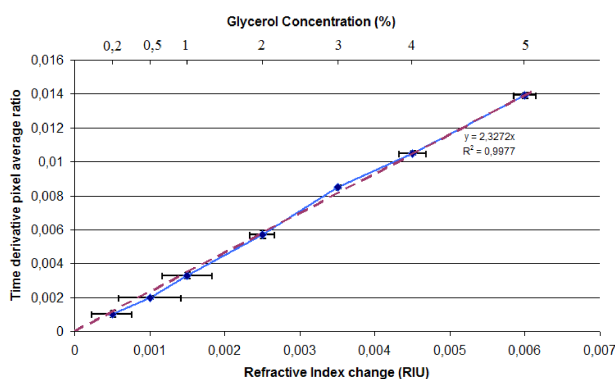


Fig. 6. Trend of the time derivative pixel average ratios vs. refractive index change. Distilled water ($n = 1,333$) was assumed as reference. Biochip model B1001-13b was used.

Each experiment was repeated three times to assure measurements repeatability and the pixel average values are filtered with a moving average filter to eliminate outliers during the acquisitions.

The refractive index change was measured as the difference between the refractive index of distilled water and the solutions ones measured with an Abbe refractometer.

The correlation coefficient (R^2) of standard y-intercept and the measured data was 0.9977.

The variation of the response with respect to small changes in refractive index is caused by various factors as the detector noise and the LED fluctuations. The CMOS image sensor parameters as black level calibration and properties as the quantum efficiency at the wavelength used, may cause statistical fluctuations in the quantity of light captured. In the same way the electrical properties of the LED may affect the measurement.

Fig. 6 shows also a resolution limit for bulk refractive index respect to the baseline noise (measuring the standard deviation), equal to $\sim 10^{-5}$ RIU for a glycerol concentration of 0.2%, which corresponds to the theoretical detection limit of the biochip [24]. This value increases as the concentration to 10^{-6} RIU for a glycerol concentration of 4% that corresponds to 10^{-3} Refractive Index change. This is sufficient in many fields and biodetection applications.

Furthermore this novel method allows to exploit the entire biochip surface for achieving multiple analytes detection, by simply distributing different antibodies spots and control areas along the surface.

B. Future work

Future work will involve tests of biological samples with antibodies immobilized on the biochip surface. The goal is to

monitoring the adsorption and evaluate the real sensitivity limit for small molecule analyte detection.

Another important future step concerns the integration of the device with a microfluidic cell for the injection of the sample and the connection with a touch-screen monitor for display the signal response for the reaction kinetics observation.

VIII. CONCLUSIONS

The multiparametric SPRi biosensor described here provides efficient solution to the limit of the available SPR instrumentation, in terms of portability, power consumption, low-cost (about 1000\$) and simplicity design. This device offers a real-time analytes detection useful for a large number of applications as medical diagnostic, monitoring of food allergens, toxins and pathogens detection in water and soils without the aid of specialized research laboratories.

A simple embedded system is used to elaborate images of a nanostructured biochip surface irradiated by a IR LED. Specific modules and device drives for Linux-based operating system have been developed to manage the biosensors components.

In particular, the pixels captured by a CMOS sensor are sent to an ARM9 processor via its GPIO interface and elaborated with a novel detection method. This new approach uses the time derivative pixels average ratios to identify change of refractive index on the biochip surface. The analysis results are available on LCD display in about 14 seconds and all the information are stored in an external SD memory.

The sensitivity for bulk refractive index changes is also measured to test the biosensor potential. The results for glycerol solutions at different concentrations indicate a best resolution of 10^{-5} RIU, suitable in several applications and fields. This detected biosensor response corresponds to the biochip theoretical response estimated by [24].

The device peculiar characteristics and the results achieved so far highlight a promising direction for a massive use for on-site analysis in thirdworld countries.

ACKNOWLEDGMENTS

The authors are very thankful to prof. Alessandro Rubini for his help during the development of the ARM9 modules.

REFERENCES

- [1] Ramanavičius A., Herberg F. W., Hutschenreiter S., Zimmermann B., Lapėnaitė I., Kaušaitė A., Finkelšteinas A., Ramanavičienė A., "Biomedical application of surface plasmon resonance biosensors (review)", *Acta Medica Lituanica*, 2005, Vol. 12, No. 3, pp. 1-9.
- [2] Valsesia et al., 2013, "SPR sensor device with nanostructure", European Patent Application 11174058.5, 16/01/2013.
- [3] Hoa X. D., Kirk A. G., Tabrizian M., "Towards integrated and sensitive surface plasmon resonance biosensor: A review of recent progress", *Biosensor and Bioelectronics*, 2007, No. 23, pp. 151-160.
- [4] Chinowsky T. M., Quinn J.G., Bartholomew D.U., Kaiser R., Elkind J.L., "Performance of the Spreeta 2000 integrated surface plasmon resonance affinity sensor", *Sensor and Actuators B*, 2003, No. 91, pp. 266-274.
- [5] Koel M., Kaljurand M., "Green Analytical Chemistry", 2010, RSC Publishing, ISBN: 978-1-84755-872-5.

- [6] Chinowsky T. M., Soelberg S. D., Baker P., Swanson N. R., Kauffman P., Mactutus A., Grow M. S., Atmar R., Yee S. S., Furlong C. E., "Portable 24-analyte surface plasmon resonance instruments for rapid, versatile biodetection", *Biosensor and Bioelectronics*, 2007, Vol. 22, pp. 2268-2275.
- [7] Hu J., Hu J., Luo F., Li W., Jiang G., Li Z., Zhang R., "Design and validation of a low cost surface plasmon resonance bioanalyzer using microprocessor and a touch-screen monitor", *Biosensor and Bioelectronics*, 2009, Vol. 24, pp. 1974-1978.
- [8] Cai H., Li H., Zhang L., Chen X., Cui D., "Portable Surface Plasmon Resonance Instrument based on a Monolithic Scanner Chip", *3rd International Conference on Biomedical Engineering and Informatics*, 2010, pp. 1153-1155.
- [9] Shin Y.-B., Min Kim H., Jung Y., Chung B.H., "A new palm-sized surface plasmon resonance (SPR) biosensor based on modulation of light source by rotating mirror", *Sensor and Actuators B: Chemical*, 2010, No. 150, pp.1-6.
- [10] Weichert F., Gaspar M., Timm C., Zybin A., Gurevich E.L., Engel M., Müller H., Markwedel P., "Signal Analysis and Classification for Surface Plasmon Assisted Microscopy of Nanoobjects", *Sensor and Actuators B: Chemical*, 2010, No. 151 pp. 281-290.
- [11] Roh S., Chung T., Lee B., "Overview of the Characteristics of Micro and Nano Structured Surface Plasmon Resonance Sensors", *Sensors*, 2011, No. 11, pp. 1565-1588.
- [12] Piliarik M., Vala M., Tichý I., Homola J., "Compact and low-cost biosensor based on novel approach to spectroscopy of surface plasmons", *Biosensor and Bioelectronics*, 2009, No. 24, pp. 3430-3435.
- [13] Vala M., Chadt K., Piliarik M., Homola J., "High-performance compact SPR sensor for multi-analyte sensing", *Sensor and Actuators B: Chemical*, 2010, No. 148, pp. 544-549.
- [14] Green J. R., Frazier A. R., Shakesheff M. K., Davies C. M., Roberts J. C., Tendler J.B. S., "Surface plasmon resonance analysis of dynamical biological interactions with biomaterials", *Biomaterials*, 2000, Vol. 21, pp. 1823-1835.
- [15] Homola J., "Surface Plasmon Resonance Sensor for Detection of Chemical and Biological Species", *Chemical Reviews*, 2008, Vol. 108, pp. 462-493.
- [16] Hutter E., Fendler H. J., "Exploitation of Localized Surface Plasmon Resonance", *Advanced Material*, 2004, Vol. 16, No. 19, pp. 1685-1706.
- [17] Zhao J., Zhang X., Yonzon C. R., Haes J. A., Van Duyne P. R., "Localized surface plasmon resonance biosensor", 2006, *Future Medicine Ltd*, No.1, pp. 219-228.
- [18] Byun K.-M., "Development of nanostructured plasmonic substrates for enhanced optical biosensing", *J. Opt. Soc. Kor.*, 2010, No. 2, Vol. 14, pp. 65-76.
- [19] Parsons J., Hendry E., Burrows C.P., Auguie B., Sambles J. R., Barnes W., L., "Localized surface-plasmon resonance in periodic nondiffracting metallic nanoparticle and nanohole arrays", *Physical Review B*, 2009, Vol. 79, Issue 7, 073412.
- [20] Lesuffleur A., Im H., Lindquist N. C., Lim S. K., Oh S., "Plasmonic Nanohole Arrays for Real-Time Multiplexing Biosensing", *Biosensing*, 2008, Vol. 7035, 703504-1.
- [21] De Leebeek A., Kumar S. L. K., De Lange V., Sinton D., Gordon R., Brolo A. G., "On-Chip SurfaceBased Detection with Nanohole Arrays", *Analytical Chemistry*, 2007, Vol. 79, No. 11, pp. 4094-4100.
- [22] Eftekhari F., Ferreira J., Santos M. L. J., Escobedo C., Brolo A. G., Sinton D., Gordon R., "Development of Portable SPR Sensor Devices Based on integrated Periodic Arrays of Nanoholes", *Optical Sensors*, 2009, Vol. 7356, 73560C-1.
- [23] Im H., Sutherland J. N., Maynard J. A., Oh S., "Nanohole-based SPR Instruments with Improved Spectral Resolution Quantify a Broad Range of Antibody-Ligand Binding Kinetics", *Analytical Chemistry*, 2012, Vol. 84(4), pp. 1941-1947.
- [24] Giudicatti S., Valsesia A., Marabelli F., Colpo P., Rossi F., "Plasmonic resonance in nanostructured gold/polymer surfaces by colloidal lithography", *Physica Status Solidi A*, 2010, Vol. 207, No. 4, pp. 935-942.
- [25] Carlson, B.S., "Comparison of modern CCD and CMOS image sensor technologies and systems for low resolution imaging", *Sensors*, 2002, Proceedings of IEEE, Vol.1, pp. 171- 176.
- [26] Hu J., Zhang G., "Research transplanting method of embedded linux kernel based on ARM platform", *International Conference of Information Science and Management Engineering (ISME)*, Vol. 2, pp. 35-38, 7-8 Aug. 2010.